Chapter 7
Kinetic Theory

Abstract Kinetic theory provides the basis for macroscopic state variables, such as pressure and temperature, by developing a microscopic picture of particles with kinetic energy, momentum, and, moreover, internal degrees of freedom. Thus, it follows an atomistic model. To treat a system of typically 10^{23} particles, kinetic theory introduces the concept of probability and statistics into science. (The probability concept is, moreover, key to the description of quantum mechanics. However, we must clearly distinguish between *thermodynamic* probability introduced by Ludwig Boltzmann and *quantum mechanical* probability resulting from Max Born's interpretation of the wave function (see Sect. 9.1.2 on page 216).) Among the probability density functions, the Maxwell-Boltzmann distribution for the particle velocity is the most prominent, and we deal with it in several problems. The characteristics of a molecular beam leaving an effusion cell, in addition to film growth, are further examples that demonstrate the practical use of kinetic theory.

7.1 Basic Concepts

In the following, it is assumed that the reader is familiar with the basic principles of classical mechanics.

7.1.1 Maxwell-Boltzmann Velocity Distribution

Strictly speaking, thermodynamics can be formulated without a fundamental concept of the nature of matter. The atomistic concept worked out by John Dalton and Amedeo Avogadro, however, is fundamental to chemistry. Textbooks demonstrate how pressure and the equation of state of a perfect gas can be traced back to the statistical movement of microscopic particles making elastic collisions with system walls (see Fig. 7.1). The **Maxwell-Boltzmann** velocity distribution can be chosen

J. Vogt, *Exam Survival Guide: Physical Chemistry*,
DOI 10.1007/978-3-319-49810-2_7

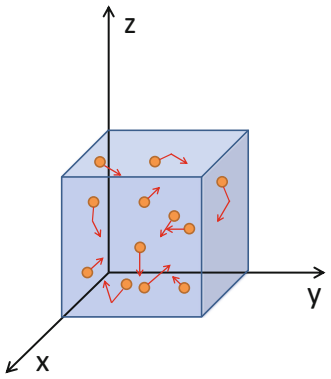

Fig. 7.1 Microscopic model of a gas within a box

as a basis. It states that at a temperature T the fraction $\frac{dN(\mathbf{v})}{N_{\text{tot}}}$ of particles of mass m with a velocity between $\mathbf{v}$ and $\mathbf{v} + d\mathbf{v}$ is

$$\frac{dN(\mathbf{v})}{N_{\text{tot}}} = \left(\frac{m}{2\pi k_B T}\right)^{\frac{3}{2}} \exp\left(-\frac{mv^2}{2k_B T}\right) d\mathbf{v}, \tag{7.1}$$

where N_{tot} is the total number of particles, and $k_B = 1.3806488 \times 10^{-23}\,\text{J}\,\text{K}^{-1}$ is the Boltzmann constant (see Sect. A.1). This distribution follows from very general assumptions, such as the homogeneity and the isotropy of the system. Note that the Maxwell-Boltzmann distribution assumes thermal equilibrium, which in many situations may not be established.

7.1.2 Pressure

The microscopic picture (Fig. 7.1) gives the relationship between the velocity of the particles and pressure p. The assumption of elastic collisions of particles with the system walls and momentum conservation yields:

$$p = \frac{1}{3}\mathcal{N} m \langle v^2 \rangle \tag{7.2}$$

where $\mathcal{N}$ is the number of particles per volume, m is their mass, and $\langle v^2 \rangle$ their mean square velocity resulting from Eq. (7.1).

7.1.3 Collisions Between Particles

The total collision frequency Z_{AB} between N_A particles of types A and N_B particles of type B depends on the **cross-section** σ_{AB}, their masses m_A and m_B, and temperature:

$$Z_{AB} = N_A N_B \sigma_{AB} \left(\frac{8 k_B T}{\mu} \right)^{\frac{1}{2}}, \tag{7.3}$$

where

$$\mu = \frac{m_A m_B}{m_A + m_B} \tag{7.4}$$

is the **effective mass**. In the simplest case of elastic collisions of rigid spherical particles with diameters d_A and d_B, the cross-sectional area is that of a disk of *radius* $d_{AB} = \frac{1}{2}(d_A + d_B)$ (see Fig. 7.2):

$$\sigma_{AB} = \pi d_{AB}^2 \tag{7.5}$$

Equation (7.3) is based on the summation of the z_{AB} individual collisions of N_A particles of type A with type B. To calculate z_{AB}, it is tentatively assumed that all particles are at rest, except for one of type A sweeping through the gas with the mean velocity $\langle v_A \rangle$. A collision with a particle of type B occurs if it is passed by the moving particle at a distance less than or equal to d_{AB} (see Fig. 7.2), i.e., within the cross-sectional area σ_{AB}. The latter defines the basal plane of the cylindrical volume $\sigma_{AB} \langle v_A \rangle$, which the moving particle passes per unit of time.

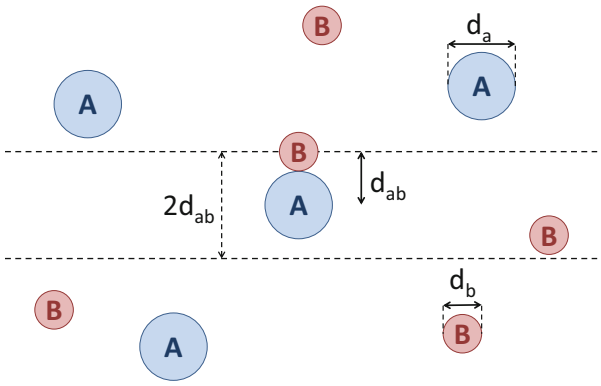

Fig. 7.2 Collisions between particles in a mixture of perfect gases of types A and B, treated within the *hard sphere model*. Collisions of the particle in the center occur with all particles within a cylindrical volume with a cross-sectional area πd_{AB}^2

Given the particle density $\mathcal{N}_B$ of type B particles, the moving particle collides with $\sigma_{AB}\langle v_A\rangle\mathcal{N}_B$ particles of type B. The picture, however, is incorrect because all particles are in permanent movement. Therefore, the mean velocity of particle A is replaced by the mean *relative* velocity $\langle v_{AB}\rangle$ of the particles. Therefore, the collision frequency of one particle of type A with particles of type B is

$$z_{AB} = \sigma_{AB}\langle v_{AB}\rangle\mathcal{N}_B \tag{7.6}$$

The somewhat tedious calculation of $\langle v_{AB}\rangle$ is treated in Problem 7.3. The result is

$$\langle v_{AB}\rangle = \left(\frac{8k_BT}{\pi\mu}\right)^{\frac{1}{2}}. \tag{7.7}$$

From the collision frequency of a particle of type A, its **mean free path** λ_A between two collisions results:

$$\lambda_A = \frac{\langle v_A\rangle}{z} \tag{7.8}$$

Here z is the number of collisions the particle experiences per unit of time.

7.1.4 Collisions with Surfaces

The rate at which particles collide with a surface is key for gas surface interactions, such as scattering, adsorption, and film growth processes. Moreover, the number of particles that strike a certain surface area per second is also an important quantity for dealing with gas effusion through a small orifice. A rigorous calculation found in many textbooks shows that the impingement rate I, i.e., the number of particles striking a surface element dA in the time dt is related to the mean velocity at a given temperature:

$$I = \frac{N}{dA\,dt} = \frac{1}{4}\mathcal{N}\langle v\rangle \tag{7.9}$$

Very often, the impingement rate is expressed in terms of pressure, which can be related to $\mathcal{N}$ via the equation of state: $p = \mathcal{N}k_BT$. Moreover, as shown in Problem 7.1 (Eq. (7.16)), the assumption of a Maxwell-Boltzmann distribution of the gas particles with mass m leads to $\langle v\rangle = \left(\frac{8k_BT}{\pi m}\right)^{\frac{1}{2}}$. Thus,

$$I = \frac{p}{\sqrt{2\pi mk_BT}} \tag{7.10}$$

7.2 Problems

Problem 7.1 (Maxwell-Boltzmann Distribution I)

a. Write down explicit expressions of the Maxwell-Boltzmann distribution in Cartesian coordinates, polar coordinates, and cylindrical coordinates (*Hint: useful information on polar and cylindrical coordinates can be found in the appendix in Sects. A.3.11 and A.3.12*).
b. Prove that the Maxwell-Boltzmann distribution (Eq. (7.1)) is normalized, i.e.,

$$\int_{\text{all molecules}} \frac{dN(\mathbf{v})}{N_{\text{tot}}} = 1 \tag{7.11}$$

c. Provide expressions for the average speed $\langle v \rangle$, the mean square speed $\langle v^2 \rangle$, and the velocity at which the distribution takes its maximum value. Give explicit values of these quantities for helium gas at 300 K and at 1,000 K.

Solution 7.1 In this problem, we familiarize ourselves with the Maxwell-Boltzmann distribution function for the velocity of particles in a gas. The velocity of a single particle is a vector. In the absence of conditions that would define a preferred direction, however, the gas is an isotropic system. This must also be reflected in the various forms of the Maxwell-Boltzmann distribution using different sets of coordinates.

In **subproblem (a)**, we give expressions for the distribution using different choices of coordinates. In **Cartesian coordinates**, the velocity squared is $v^2 = v_x^2 + v_y^2 + v_z^2$, where v_x, v_y, and v_z are the velocity in x-, y-, and z-direction respectively. Hence,

$$\frac{dN(v_x, v_y, v_z)}{N_{\text{tot}}} = \left(\frac{m}{2\pi k_B T}\right)^{\frac{3}{2}} \exp\left(-\frac{m}{2k_B T}\left(v_x^2 + v_y^2 + v_z^2\right)\right) dv_x\, dv_y\, dv_z \tag{7.12}$$

Apparently, the distribution function is separable, i.e.,

$$\frac{dN(v_x, v_y, v_z)}{N_{\text{tot}}} = f(v_x) f(v_y) f(v_z)\, dv_x\, dv_y\, dv_z$$

and for each Cartesian component, the same symmetric Gaussian distribution function holds:

$$f(v_x) = \left(\frac{m}{2\pi k_B T}\right)^{\frac{1}{2}} \exp\left(-\frac{m}{2k_B T} v_x^2\right) \tag{7.13}$$

In many problems, however, **spherical coordinates** (see Sect. A.3.11) are the suitable choice. The velocity vector is characterized by its scalar value v, and the direction expressed by a polar angle θ and the azimuthal angle ϕ. We obtain:

$$\frac{dN(v,\theta,\phi)}{N_{\text{tot}}} = \left(\frac{m}{2\pi k_B T}\right)^{\frac{3}{2}} \exp\left(-\frac{mv^2}{2k_B T}\right) v^2 \sin\theta \, dv \, d\theta \, d\phi \tag{7.14}$$

In some cases, **cylindrical coordinates** (see Sect. A.3.12) are appropriate. Apart from a velocity component v_z in the z direction, a velocity component v_r perpendicular to the z axis and an azimuthal angle ϕ is considered. We obtain:

$$\frac{dN(v_z, v_r, \phi)}{N_{\text{tot}}} = \left(\frac{m}{2\pi k_B T}\right)^{\frac{3}{2}} \exp\left(-\frac{m}{2k_B T}\left(v_z^2 + v_r^2\right)\right) v_r \, dv_z \, dv_r, d\phi \tag{7.15}$$

In **subproblem (b)**, we check the normalization of the Maxwell-Boltzmann distribution by integrating over the entire velocity space. We are free to choose one of the coordinate systems and select spherical coordinates (Eq. (7.14)). The integral in Eq. (7.11) can be separated in a product of three integrals. Using the integrals given in Sect. A.3.7 in the appendix, we obtain:

$$\int_{\text{all molecules}} \frac{dN(\mathbf{v})}{N_{\text{tot}}} = \left(\frac{m}{2\pi k_B T}\right)^{\frac{3}{2}} \underbrace{\int_0^\infty v^2 \exp\left(-\frac{mv^2}{2k_B T}\right) dv}_{= \frac{\sqrt{\pi}}{4\left(\frac{m}{2k_B T}\right)^{\frac{3}{2}}} \text{ (see Eq. (A.47))}} \underbrace{\int_0^\pi \sin\theta d\theta}_{= 2 \text{ (see Eq. (A.39))}} \underbrace{\int_0^{2\pi} d\phi}_{= 2\pi}$$

$$= 1$$

Hence, the distribution is normalized and we can use it to calculate expectation values of relevant quantities, such as the average speed $\langle v \rangle$ of the particles, as we do in **subproblem (c)**. In Fig. 7.3 the velocity distribution of helium is shown for two temperatures, 300 K and 1,000 K respectively. We notice the asymmetry of the curves. The high velocity tail is wider than at low velocities.

$$\langle v \rangle = \int_{\text{all molecules}} v \frac{dN(v,\theta,\phi)}{N_{\cdot tot}} = 4\pi \left(\frac{m}{2\pi k_B T}\right)^{\frac{3}{2}} \int_0^\infty v^3 \exp\left(-\frac{mv^2}{2k_B T}\right) dv$$

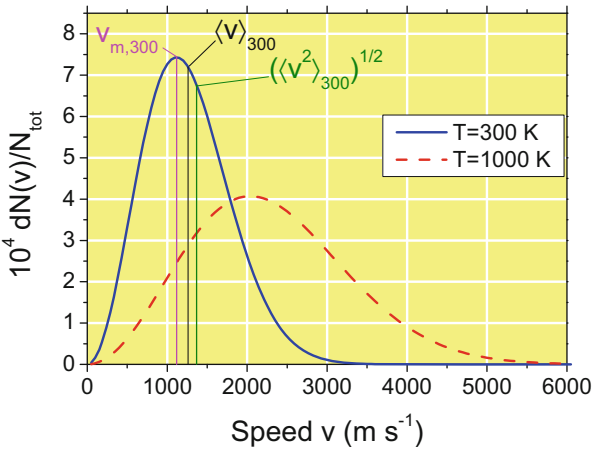

Fig. 7.3 Maxwell-Boltzmann velocity distribution for helium near room temperature (*solid line*) and at 1,000 K (*dashed line*). As shown for $T = 300$ K, the maximum of the distribution v_m, the average speed $\langle v \rangle$, and the root mean square velocity $\sqrt{\langle v^2 \rangle}$ take different values because the distribution is asymmetric

The integral is evaluated using the integral table in the appendix (Eq. (A.48)). We obtain:

$$\langle v \rangle = 4\pi \left(\frac{m}{2\pi k_B T} \right)^{\frac{3}{2}} \frac{2k_B^2 T^2}{m^2} = \left(\frac{8k_B T}{\pi m} \right)^{\frac{1}{2}} \tag{7.16}$$

The noble gas helium has an atomic mass $4m_u = 6.64 \times 10^{-27}$ kg. At a temperature of 300 K, its average speed is thus 1260 m s^{-1}. At a temperature of 1,000 K, $\langle v \rangle$ is 2300 m s^{-1}. For the mean square speed $\langle v^2 \rangle$, we obtain:

$$\langle v^2 \rangle = \int_{\text{all molecules}} v^2 \frac{dN(v, \theta, \phi)}{N_{\text{tot}}} = 4\pi \left(\frac{m}{2\pi k_B T} \right)^{\frac{3}{2}} \int_0^\infty v^4 \exp\left(-\frac{mv^2}{2k_B T} \right) dv$$

Using the integral table (Eq. (A.49)), we obtain:

$$\langle v^2 \rangle = 4\pi \left(\frac{m}{2\pi k_B T} \right)^{\frac{3}{2}} \frac{3\sqrt{\pi}}{8} \left(\frac{2k_B T}{m} \right)^{\frac{5}{2}} = \frac{3k_B T}{m} \tag{7.17}$$

At a temperature of 300 K, the mean square velocity of helium is thus 1.87×10^6 m^2 s^{-2}; the root mean square velocity $\sqrt{\langle v^2 \rangle}$ is 1368 m s^{-1}. At a temperature of 1,000 K, $\langle v^2 \rangle$ reaches 6.24×10^6 m^2 s^{-2}, and $\sqrt{\langle v^2 \rangle}$ is 2497 m s^{-1}. Equation (7.17)

is an important result by which the **average kinetic energy** is obtained:

$$\langle E_{\text{kin}} \rangle = \frac{1}{2} m \langle v^2 \rangle = \frac{3}{2} k_B T \tag{7.18}$$

This expression is related to the internal energy of a monatomic perfect gas with its three translational degrees of freedom. Moreover, the result for $\langle v^2 \rangle$ inserted into Eq. (7.2) yields the equation of state of the perfect gas: $pV = N_{\text{tot}} k_B T$. Finally, we seek the most probable velocity, i.e., the maximum of the Maxwell-Boltzmann distribution. The necessary condition for the maximum is:

$$\frac{1}{N_{\text{tot}}} \frac{dN(v)}{dv} \stackrel{!}{=} 0.$$

Insertion of Eq. (7.14) yields

$$4\pi \left(\frac{m}{2\pi k_B T} \right)^{\frac{3}{2}} \left[2v \exp\left(-\frac{mv^2}{2k_B T} \right) - \frac{mv^3}{k_B T} \exp\left(-\frac{mv^2}{2k_B T} \right) \right] \stackrel{!}{=} 0.$$

For arbitrary T and m, this requires

$$2v - \frac{mv^3}{k_B T} \stackrel{!}{=} 0$$

Therefore, the velocity distribution function is a maximum of:

$$v_m = \sqrt{\frac{2k_B T}{m}}. \tag{7.19}$$

At 300 K, the maximum value of helium is $1{,}117\,\text{m}\,\text{s}^{-1}$; at 1,000 K $v_m = 2{,}039\,\text{m}\,\text{s}^{-1}$ is obtained. Our results for v_m, $\langle v \rangle$, and $\sqrt{\langle v^2 \rangle}$ are different for a given temperature, which is also illustrated in Fig. 7.3 for $T = 300\,\text{K}$. This is caused by the asymmetry of the distribution functions.

Problem 7.2 (Maxwell-Boltzmann Distribution II)

a. Prove that the Maxwell-Boltzmann velocity distribution Eq. (7.1) leads to a probability density distribution for the kinetic energy that does only depend on temperature and physical constants. Prove that the latter can be mapped to:

$$\frac{dN(\epsilon)}{N_{\text{tot}}} = \frac{2}{\sqrt{\pi}} e^{-\epsilon} \sqrt{\epsilon}\, d\epsilon \tag{7.20}$$

(continued)

Problem 7.2 (continued)

where $\epsilon = \frac{E}{k_B T}$.

b. Plot Eq. (7.20), give an interpretation of the shape of the distribution function, and determine its maximum.

c. Cumulative probabilities: show that the probability of a particle having a kinetic energy less than or equal to a certain threshold energy ϵ^* is:

$$W_c(0, \epsilon^*) = \int_{\epsilon<\epsilon^*} \frac{dN(\epsilon)}{N_{\text{tot}}} = \frac{4}{\sqrt{\pi}} \epsilon^{*\frac{3}{2}} \sum_{n=0}^{\infty} \frac{(-1)^n}{n!} \frac{1}{2n+3} \epsilon^{*n} \tag{7.21}$$

d. Use Eq. (7.21) to calculate the probability that the energy of a particle exceeds the thermal energy by a factor of 2, 3, 4, 5, and 10. Alternatively, you can use the following identity with erfc(x) being the *complementary error function*:

$$W_c(\epsilon^*, \infty) = \int_{\epsilon>\epsilon^*} \frac{dN(\epsilon)}{N_{\text{tot}}} = \frac{2}{\sqrt{\pi}} \sqrt{\epsilon^*} e^{-\epsilon^*} + \text{erfc}(\sqrt{\epsilon^*}) \tag{7.22}$$

Solution 7.2 In this exercise, we deal with the kinetic energy distribution of a gas. Classical mechanics relates the kinetic energy of a particle of mass m to its velocity v by means of:

$$E = \frac{1}{2} m v^2. \tag{7.23}$$

The derivation of the probability density distribution of the particles having a kinetic energy between E and $E + dE$ should thus be straightforward. In **subproblem (a)**, we start from the Maxwell-Boltzmann velocity distribution

$$\frac{dN(v)}{N_{\text{tot}}} = 4\pi \left(\frac{m}{2\pi k_B T} \right)^{\frac{3}{2}} v^2 \exp\left(-\frac{mv^2}{2k_B T} \right) dv \tag{7.24}$$

We make a substitution in the exponent according to Eq. (7.23). Moreover, we consider $dE = mv\,dv = p\,dv$ and the relation $p = \sqrt{2mE}$ between momentum p

and kinetic energy E. We obtain:

$$\frac{dN(E)}{N_{\text{tot}}} = 4\pi \left(\frac{m}{2\pi k_B T}\right)^{\frac{3}{2}} \frac{2}{m} \underbrace{\frac{mv^2}{2}}_{E} \exp\left(-\frac{E}{k_B T}\right) \underbrace{dv}_{\frac{dE}{\sqrt{2mE}}}$$

$$= 2\pi \left(\frac{2}{m}\right)^{\frac{3}{2}} \left(\frac{m}{2\pi k_B T}\right)^{\frac{3}{2}} \exp\left(-\frac{E}{k_B T}\right) \sqrt{E}\, dE$$

Therefore,

$$\frac{dN(E)}{N_{\text{tot}}} = 2\pi \left(\frac{1}{\pi k_B T}\right)^{\frac{3}{2}} \exp\left(-\frac{E}{k_B T}\right) \sqrt{E}\, dE \tag{7.25}$$

The last equation shows that the energy distribution is independent of the particle mass and only depends on temperature, as expected for a perfect gas (compare also Eq. (7.18) in Problem 7.1). The exponent suggests a special scaling of energy in units of the thermal energy $k_B T$ at an arbitrary given temperature. Thus, we define the dimensionless quantity $\epsilon = \frac{E}{k_B T}$. Accordingly, we use $dE = k_B T\, d\epsilon$ and obtain:

$$\frac{dN(\epsilon)}{N_{\text{tot}}} = 2\pi \left(\frac{1}{\pi k_B T}\right)^{\frac{3}{2}} \exp(-\epsilon) \underbrace{\sqrt{\frac{E}{k_B T}}}_{\sqrt{\epsilon}} \sqrt{k_B T} \underbrace{dE}_{k_B T\, d\epsilon}$$

$$= \frac{2}{\sqrt{\pi}} e^{-\epsilon} \sqrt{\epsilon}\, d\epsilon$$

The last line proves Eq. (7.20). The resulting probability density function

$$w(\epsilon) = \frac{2}{\sqrt{\pi}} e^{-\epsilon} \sqrt{\epsilon}, \tag{7.26}$$

to be plotted in **subproblem (b)** is shown in Fig. 7.4. The distribution is clearly asymmetric with a steeply rising probability density in the low-energy tail. Gas particles with low kinetic energy are apparently very rare in the situation of thermal equilibrium, where collisions among particles rapidly distribute the energy. A particle at rest is rapidly *kicked* by some other molecule. On the other hand, inspection of Fig. 7.4 leads to the qualitative conclusion that the number of molecules with an energy above the thermal energy ($\epsilon > 1$) is quite high and

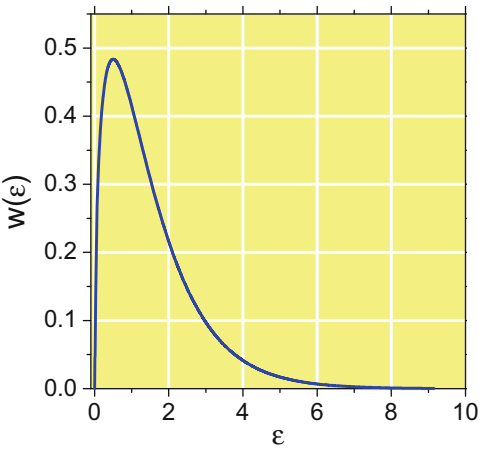

Fig. 7.4 Probability density function for the kinetic energy ϵ of a perfect gas scaled to the thermal energy according to Eq. (7.26)

we seek quantitative results in our next steps. At first, it is easy to determine the maximum of $w(\epsilon)$ by taking the necessary condition for a maximum, i.e., the first derivative of $w(\epsilon)$ must be zero:

$$\frac{d\,w(\epsilon)}{d\epsilon} \overset{\text{Eq. (A.15)}}{=} \frac{2}{\sqrt{\pi}}\left[\frac{1}{2\sqrt{\epsilon}} - \sqrt{\epsilon}\right] e^{-\epsilon} \overset{!}{=} 0$$

This requires the bracket to vanish, which happens for $\epsilon_{\max} = \frac{1}{2}$, where $w(\epsilon_{\max}) = 0.48$.

Next, we deal with the calculation of *cumulative probabilities* in **subproblem (c)**, i.e., the probability that the energy of a particle falls within a certain range. For example, cumulative probabilities of particles, whose kinetic energy is higher than a specific activation energy, influence the reaction rate if one assumes that the activation of a particle is mediated by collisions. To calculate such probabilities, we have to integrate Eq. (7.26) with arbitrary integration limits, but for this purpose we must find the primitive of $w(\epsilon)$. We use a power series ansatz to calculate cumulative probabilities and start with:

$$W_c(0, \epsilon^*) = \int_{\epsilon<\epsilon^*} \frac{d\,N(\epsilon)}{N_{\text{tot}}} = \int_0^{\epsilon^*} w(\epsilon)\,d\epsilon = \int_0^{\epsilon^*} \frac{2}{\sqrt{\pi}} e^{-\epsilon}\sqrt{\epsilon}\,d\epsilon, \tag{7.27}$$

which gives the fraction of molecules with an energy between zero and ϵ^*. We write the exponential function as a power series (see appendix Eq. (A.55)) and obtain:

$$W_c(0, \epsilon^*) = \frac{2}{\sqrt{\pi}} \int_0^{\epsilon^*} \epsilon^{\frac{1}{2}} \sum_{n=0}^{\infty} \frac{(-1)^n \epsilon^n}{n!}\,d\epsilon,$$

Then, the strategy is to make the integration piecewise for every member of the sum:

$$W_c(0,\epsilon^*) = \frac{2}{\sqrt{\pi}} \sum_{n=0}^{\infty} \frac{(-1)^n}{n!} \int_0^{\epsilon^*} \epsilon^{n+\frac{1}{2}}\, d\epsilon, = \frac{2}{\sqrt{\pi}} \sum_{n=0}^{\infty} \frac{(-1)^n}{n!} \frac{1}{n+\frac{3}{2}} \epsilon^{n+\frac{3}{2}} \Big|_0^{\epsilon^*}$$

We thus obtain:

$$W_c(0,\epsilon^*) = \int_{\epsilon<\epsilon^*} \frac{dN(\epsilon)}{N_{\text{tot}}} = \frac{4}{\sqrt{\pi}} \epsilon^{*\frac{3}{2}} \sum_{n=0}^{\infty} \frac{(-1)^n}{n!} \frac{1}{2n+3} \epsilon^{*n} \tag{7.28}$$

which proves Eq. (7.21). Is this equation applicable? This depends on the convergence of the series.

In **subproblem (d)**, we check this by experience. We set up a simple computer routine that, starting from the first term for $n = 0$, repeatedly calculates the next member of the series and adds it to the sum, until a certain convergence limit κ is reached. For a given index n with $a_n = \frac{(-1)^n}{n!} \frac{1}{2n+3} \epsilon^{*n}$, the next member of the sequence is easily calculated using the following method: $a_{n+1} = -\frac{a_n \epsilon^*}{(n+1)(2n+5)}$. Proceeding in this way avoids the repeated expensive calculation of factorials $n!$. If we were to choose a convergence criterion of $\kappa = 10^{-9}$, convergence would be reached after the summation up to $n = 12$ for $\epsilon^* = 1$. For larger values of ϵ^* more terms would have to be added. For $\epsilon^* = 10$ we would need to add 40 terms to reach convergence.

For values of ϵ^* up to 10, the results obtained with Eq. (7.28) are depicted in Fig. 7.5 (red curve). Starting from zero, the $W_c(0,\epsilon^*)$ raises and reaches a saturation value of 1, corresponding to the expected normalization of the probability density distribution $w(\epsilon)$. The solid curve in Fig. 7.5 illustrates the

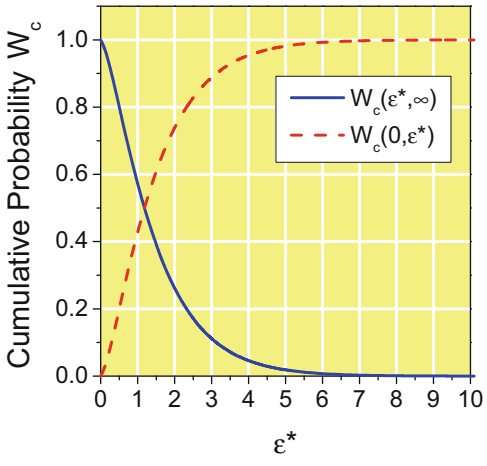

Fig. 7.5 Cumulative probability for particles with a kinetic energy below a threshold value ϵ^* ($W_c(0,\epsilon^*)$, *dashed curve*), or above ϵ^* ($W_c(\epsilon^*,\infty)$, *solid curve*)

Table 7.1 Cumulative probability $W_c(\epsilon^*, \infty)$ of particles with energies above several multiples of the thermal energy, ϵ^*

ϵ^*	2	3	4	5	10
$W_c(\epsilon^*, \infty)$	0.261	0.112	0.046	0.019	1.7×10^{-4}

See also the solid curve in Fig. 7.5

reversed cumulative probability of finding a particle with kinetic energy above the threshold value, $W_c(\epsilon^*, \infty) = 1 - W_c(0, \epsilon^*)$. It is unity for $\epsilon^* = 0$ and reaches a saturation value of zero. It can be shown that $W_c(\epsilon^*, \infty)$ is obtained using Eq. (7.22). The complimentary error function $\mathrm{erfc}(x) = 1 - \mathrm{erf}(x)$ used in this equation is implemented by standard mathematical software packages. It is calculated numerically by a power series (see Eq. (A.60) in the appendix). Using the function $W_c(\epsilon^*, \infty)$, we can determine the sought probabilities of particles having energies above numerous threshold values. These probabilities are summarized in Table 7.1. More than 26% of the particles in a perfect gas have a kinetic energy that is twice the thermal energy at equilibrium. The energy of nearly 2% of the particles exceeds the thermal energy fivefold.

Problem 7.3 (Relative Velocity of Two Particles) In classical mechanics the kinetic energy of a particle of mass m moving at velocity v is $E = \frac{mv^2}{2}$.

a. Prove that the total kinetic energy of two particles A and B moving with the velocities v_A and v_B can be written

$$E_{\mathrm{tot}} = \frac{M v_{\mathrm{COM}}^2}{2} + \frac{\mu v_{\mathrm{rel}}^2}{2} \tag{7.29}$$

M is the total mass of the two particles, $\mathbf{v}_{\mathrm{COM}}$ is the velocity vector of their center of mass, $\mathbf{v}_{\mathrm{rel}} = \mathbf{v}_B - \mathbf{v}_A$ is the relative velocity vector, and μ is the effective mass (Eq. (7.4)).

b. Based on Eq. (7.29) and the Maxwell-Boltzmann velocity distribution for both types of particles, determine the mean relative velocity $\langle v_{AB} \rangle$.

Solution 7.3 This problem is related to interatomic or intermolecular collision rates (Sect. 7.1.3, Eqs. (7.3) and (7.6) respectively). In **subproblem (a)**, we use classical mechanics and vector calculus to prove that the kinetic energy of two particles A and B moving with the velocity vectors $\mathbf{v}_A$ and $\mathbf{v}_B$ can be written as the sum of the

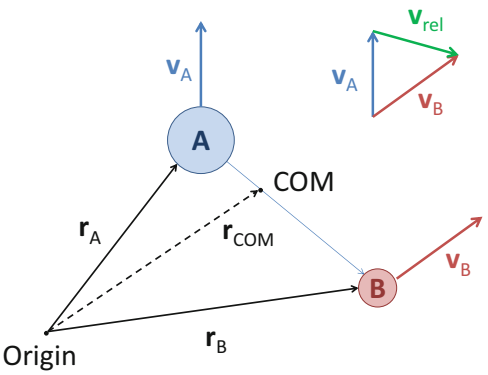

Fig. 7.6 Center of mass (COM) and relative velocity of two particles A and B located at $\mathbf{r}_A(t)$ and $\mathbf{r}_B(t)$ moving with velocities $\mathbf{v}_A$ and $\mathbf{v}_B$

kinetic energy of their center of mass (COM),

$$\mathbf{r}_{COM}(t) = \frac{m_A \mathbf{r}_A(t) + m_B \mathbf{r}_B(t)}{m_A + m_B}, \tag{7.30}$$

and a second kinetic energy term containing the relative velocity squared of the two particles and an effective mass μ. The situation is illustrated in Fig. 7.6. The center of mass is located between the two particles. Its velocity vector is obtained by differentiation of Eq. (7.30):

$$\mathbf{v}_{COM} = \frac{d\,\mathbf{r}_{COM}(t)}{dt} = \frac{m_A \mathbf{v}_A(t) + m_B \mathbf{v}_B(t)}{M}, \tag{7.31}$$

The total kinetic energy of the two particles, on the one hand, is the sum of the individual kinetic energies of the particles, i.e.,

$$E_{tot} = \frac{m_A v_A^2}{2} + \frac{m_B v_B^2}{2} \tag{7.32}$$

We could start from this last expression by ingeniously expanding both fractions, but it seems easier to start from the right-hand side of Eq. (7.29):

$$\begin{aligned}\frac{M v_{COM}^2}{2} + \frac{\mu v_{rel}^2}{2} &\overset{\text{Eq. (7.31)}}{=} \frac{M}{2}\left(\frac{m_A}{M}\mathbf{v}_A + \frac{m_B}{M}\mathbf{v}_B\right)^2 + \frac{1}{2}\frac{m_a m_B}{M}(\mathbf{v}_B - \mathbf{v}_A)^2 \\ &= \frac{M}{2}\left(\frac{m_A^2}{M^2}v_A^2 + \frac{m_B^2}{M^2}v_B^2 + \frac{2m_A m_B}{M^2}\mathbf{v}_A\mathbf{v}_B\right) \\ &\quad + \frac{m_A m_B}{2M}\left(v_A^2 + v_B^2 - 2\mathbf{v}_A\mathbf{v}_B\right)\end{aligned}$$

The two terms containing the scalar product $\mathbf{v}_\mathrm{A}\mathbf{v}_\mathrm{B}$ cancel each other out. We obtain:

$$\begin{aligned}\frac{Mv_\mathrm{COM}^2}{2}+\frac{\mu v_\mathrm{rel}^2}{2} &= \frac{1}{2}\left(\frac{m_\mathrm{A}^2}{M}v_\mathrm{A}^2+\frac{m_\mathrm{B}^2}{M}v_\mathrm{B}^2+\frac{m_\mathrm{A}m_\mathrm{B}}{M}v_\mathrm{A}^2+\frac{m_\mathrm{A}m_\mathrm{B}}{M}v_\mathrm{B}^2\right)\\ &= \frac{1}{2}\left(\frac{m_\mathrm{A}^2}{M}+\frac{m_\mathrm{A}m_\mathrm{B}}{M}\right)v_\mathrm{A}^2+\frac{1}{2}\left(\frac{m_\mathrm{B}^2}{M}+\frac{m_\mathrm{A}m_\mathrm{B}}{M}\right)v_\mathrm{B}^2\\ &= \frac{m_\mathrm{A}}{2}\left(\frac{m_\mathrm{A}+m_\mathrm{B}}{M}\right)v_\mathrm{A}^2+\frac{m_\mathrm{B}}{2}\left(\frac{m_\mathrm{A}+m_\mathrm{B}}{M}\right)v_\mathrm{B}^2\\ &= \frac{m_\mathrm{A}v_\mathrm{A}^2}{2}+\frac{m_\mathrm{B}v_\mathrm{B}^2}{2}\\ &\overset{\text{Eq. (7.32)}}{=} E_\mathrm{tot}\end{aligned}$$

It is worth mentioning that Eq. (7.29), which we have just proven, is used extensively in the treatment of two-body problems.[1] Usually, the origin in Fig. 7.6 in the center of mass is chosen and thus a separation from the kinetic energy of the center of mass from the energy of the *internal* degrees of freedom.

In **subproblem (b)** the mean relative velocity $\langle v_\mathrm{AB}\rangle$ is computed under the assumption of the Maxwell-Boltzmann velocity distribution Eq. (7.1) for both types of particles. The relative velocity is:

$$v_\mathrm{AB}=|\mathbf{v}_\mathrm{B}-\mathbf{v}_\mathrm{A}|=\sqrt{(v_{\mathrm{B},x}-v_{\mathrm{A},x})^2+\left(v_{\mathrm{B},y}-v_{\mathrm{A},y}\right)^2+(v_{\mathrm{B},z}-v_{\mathrm{A},z})^2}. \tag{7.33}$$

The expectation value is thus obtained:

$$\begin{aligned}\langle v_\mathrm{AB}\rangle = &\left(\frac{m_\mathrm{A}}{2\pi k_B T}\right)^{\frac{3}{2}}\left(\frac{m_\mathrm{B}}{2\pi k_B T}\right)^{\frac{3}{2}}\iiint_\mathrm{A}\iiint_\mathrm{B} dv_{\mathrm{A},x}dv_{\mathrm{A},y}dv_{\mathrm{A},z}dv_{\mathrm{B},x}dv_{\mathrm{B},y}dv_{\mathrm{B},z}\\ &\sqrt{(v_{\mathrm{B},x}-v_{\mathrm{A},x})^2+\left(v_{\mathrm{B},y}-v_{\mathrm{A},y}\right)^2+(v_{\mathrm{B},z}-v_{\mathrm{A},z})^2}\\ &\mathrm{e}^{\left[-\frac{m_\mathrm{A}\left(v_{\mathrm{A},x}^2+v_{\mathrm{A},y}^2+v_{\mathrm{A},z}^2\right)}{2k_BT}\right]}\mathrm{e}^{\left[-\frac{m_\mathrm{B}\left(v_{\mathrm{B},x}^2+v_{\mathrm{B},y}^2+v_{\mathrm{B},z}^2\right)}{2k_BT}\right]}\end{aligned} \tag{7.34}$$

where the triple integral over all Cartesian velocity components of the particles A and B is from $-\infty$ to $+\infty$ respectively. In the next step, we make a transformation from the six Cartesian velocity components of particle A and particle B to the three velocity components of the center of mass, $v_{\mathrm{COM},x}$, $v_{\mathrm{COM},y}$, $v_{\mathrm{COM},z}$, and the three

[1] Text book examples of two-body problems are, for example, the hydrogen problem or the rigid rotator.

relative velocity components $v_{\mathrm{rel},x}$, $v_{\mathrm{rel},y}$, and $v_{\mathrm{rel},z}$:

$$v_{\mathrm{COM},i} = \frac{m_\mathrm{A} v_{\mathrm{A},i} + m_\mathrm{B} v_{\mathrm{B},i}}{m_\mathrm{A} + m_\mathrm{B}} \qquad i = x, y, z \tag{7.35}$$

$$v_{\mathrm{AB},i} = v_{\mathrm{B},i} - v_{\mathrm{A},i} \qquad i = x, y, z \tag{7.36}$$

The apparent advantage is that the root in Eq. (7.34) only contains the three relative velocity components. Based on the results of subproblem (a), the Boltzmann factors can be transformed in:

$$\begin{aligned} &\exp\left[-\frac{m_\mathrm{A}\left(v_{\mathrm{A},x}^2 + v_{\mathrm{A},y}^2 + v_{\mathrm{A},z}^2\right)}{2k_B T}\right] \exp\left[-\frac{m_\mathrm{B}\left(v_{\mathrm{B},x}^2 + v_{\mathrm{B},y}^2 + v_{\mathrm{B},z}^2\right)}{2k_B T}\right] \\ &= \exp\left[-\frac{M\left(v_{\mathrm{COM},x}^2 + v_{\mathrm{COM},y}^2 + v_{\mathrm{COM},z}^2\right)}{2k_B T}\right] \exp\left[-\frac{\mu\left(v_{\mathrm{AB},x}^2 + v_{\mathrm{AB},y}^2 + v_{\mathrm{AB},z}^2\right)}{2k_B T}\right] \end{aligned} \tag{7.37}$$

Finally, we must consider the differentials. Evaluation of the *Jacobian* (see appendix Sect. A.3.6.1) yields the result that:

$$dv_{\mathrm{A},x} dv_{\mathrm{A},y} dv_{\mathrm{A},z} dv_{\mathrm{B},x} dv_{\mathrm{B},y} dv_{\mathrm{B},z} = dv_{\mathrm{COM},x} dv_{\mathrm{COM},y} dv_{\mathrm{COM},z} dv_{\mathrm{AB},x} dv_{\mathrm{AB},y} dv_{\mathrm{AB},z}$$

To prove this, we consider, for example, the x components $v_{\mathrm{COM},x}$ and $v_{\mathrm{AB},x}$. With Eqs. (7.35) and (7.36) we obtain:

$$\frac{\partial\left(v_{\mathrm{COM},x}, v_{\mathrm{AB},x}\right)}{\partial\left(v_{\mathrm{A},x}, v_{\mathrm{B},x}\right)} = \begin{vmatrix} \frac{\partial v_{\mathrm{COM},x}}{\partial v_{\mathrm{A},x}} & \frac{\partial v_{\mathrm{AB},x}}{\partial v_{\mathrm{A},x}} \\ \frac{\partial v_{\mathrm{COM},x}}{\partial v_{\mathrm{B},x}} & \frac{\partial v_{\mathrm{AB},x}}{\partial v_{\mathrm{B},x}} \end{vmatrix} = \begin{vmatrix} \frac{m_\mathrm{A}}{m_\mathrm{A}+m_\mathrm{B}} & -1 \\ \frac{m_\mathrm{B}}{m_\mathrm{A}+m_\mathrm{B}} & +1 \end{vmatrix} = \frac{m_\mathrm{A} + m_\mathrm{B}}{m_\mathrm{A} + m_\mathrm{B}} = 1 \tag{7.38}$$

For the other components, we obtain the same results and thus the entire Jacobian is unity. Therefore, we can separate the triple integral for the center of mass velocity components and obtain:

$$\begin{aligned} \langle v_\mathrm{AB} \rangle = &\frac{(m_\mathrm{A} m_\mathrm{B})^{\frac{3}{2}}}{(2\pi k_B T)^3} \iiint_\mathrm{COM} e^{-\frac{M\left(v_{\mathrm{COM},x}^2 + v_{\mathrm{COM},y}^2 + v_{\mathrm{COM},z}^2\right)}{2k_B T}} dv_{\mathrm{COM},x} dv_{\mathrm{COM},y} dv_{\mathrm{COM},z} \\ &\iiint_\mathrm{AB} \sqrt{v_{\mathrm{AB},x}^2 + v_{\mathrm{AB},y}^2 + v_{\mathrm{AB},z}^2}\, e^{-\frac{\mu\left(v_{\mathrm{AB},x}^2 + v_{\mathrm{AB},y}^2 + v_{\mathrm{AB},z}^2\right)}{2k_B T}} dv_{\mathrm{AB},x} dv_{\mathrm{AB},y} dv_{\mathrm{AB},z} \end{aligned} \tag{7.39}$$

The boundaries of the triple integrals are again $-\infty$ and ∞ for each component. The first triple integral for the center of mass components can be further separated into Gaussian integrals (see appendix Sect. A.3.7) for the Cartesian

components:

$$\int_{-\infty}^{\infty} e^{-\frac{M}{2k_BT}v_{\mathrm{COM},i}^2}\, dv_{\mathrm{COM},i} \overset{\text{Eq. (A.46)}}{=} \frac{\sqrt{\pi}}{\sqrt{\frac{M}{2k_BT}}} = \sqrt{\frac{2\pi k_BT}{M}} \qquad i = x, y, z$$

Thus, we obtain

$$\langle v_{\mathrm{AB}}\rangle = \frac{(m_{\mathrm{A}}m_{\mathrm{B}})^{\frac{3}{2}}}{(2\pi k_BT)^3}\left(\frac{2\pi k_BT}{M}\right)^{\frac{3}{2}} \iiint_{\mathrm{AB}} \sqrt{v_{\mathrm{AB},x}^2 + v_{\mathrm{AB},y}^2 + v_{\mathrm{AB},z}^2}\, e^{-\frac{\mu\left(v_{\mathrm{AB},x}^2+v_{\mathrm{AB},y}^2+v_{\mathrm{AB},z}^2\right)}{2k_BT}} dv_{\mathrm{AB},x}dv_{\mathrm{AB},y}dv_{\mathrm{AB},z} \tag{7.40}$$

The triple integral for the relative velocity components can be separated if we transform from Cartesian to spherical coordinates v_{AB}, θ, and ϕ. Because $\sqrt{v_{\mathrm{AB},x}^2 + v_{\mathrm{AB},y}^2 + v_{\mathrm{AB},z}^2} = v_{\mathrm{AB}}$ and $dv_{\mathrm{AB},x}dv_{\mathrm{AB},y}dv_{\mathrm{AB},z} = v_{\mathrm{AB}}^2\, dv_{\mathrm{AB}}d\theta d\phi$

$$\begin{aligned}\langle v_{\mathrm{AB}}\rangle &= \left(\frac{\mu}{2\pi k_BT}\right)^{\frac{3}{2}} \int_0^{\infty} v_{\mathrm{AB}}^3 e^{-\frac{\mu}{2k_BT}v_{\mathrm{AB}}^2}\, dv_{\mathrm{AB}} \underbrace{\int_0^{\pi} \sin\theta\, d\theta}_{2} \underbrace{\int_0^{2\pi} d\phi}_{2\pi} \\ &= 4\pi\left(\frac{\mu}{2\pi k_BT}\right)^{\frac{3}{2}} \int_0^{\infty} v_{\mathrm{AB}}^3 e^{-\frac{\mu}{2k_BT}v_{\mathrm{AB}}^2}\, dv_{\mathrm{AB}}\end{aligned}$$

The remaining integral for the radial velocity component can be evaluated with Eq. (A.48) from the appendix:

$$\int_0^{\infty} v_{\mathrm{AB}}^3 e^{-\frac{\mu}{2k_BT}v_{\mathrm{AB}}^2}\, dv_{\mathrm{AB}} = 2\left(\frac{k_BT}{\mu}\right)^2$$

Hence, the expression for the mean relative velocity is

$$\langle v_{\mathrm{AB}}\rangle = 4\pi\left(\frac{\mu}{2\pi k_BT}\right)^{\frac{3}{2}} 2\left(\frac{k_BT}{\mu}\right)^2 = \left(\frac{8k_BT}{\pi\mu}\right)^{\frac{1}{2}} \tag{7.41}$$

which is identical to Eq. (7.7).

Problem 7.4 (Collision Rates in a Helium-Xenon Gas Mixture) Assume the perfect gas behavior of helium and xenon and calculate both the individual collision rates and the mean free path of both species for a 50:50 mixture at room temperature with a total pressure of 1×10^{-8}, 0.1, and 10^5 Pa. The van der Waals radii of helium and xenon are 140 pm and 216 pm respectively.

Solution 7.4 Picking up the example of a gas mixture of helium and xenon, this exercise gives us an idea of the collision rates occurring in a gas at different pressures, and, moreover, the mean free paths. Such quantities are of importance, for example, for the characterization of transport processes in the gas, which depend significantly on pressure. If we assume perfect gas behavior for both species, we can relate the particle density to the total pressure by means of:

$$\mathscr{N}_{\mathrm{He}} = \mathscr{N}_{\mathrm{Xe}} = \frac{p_{\mathrm{tot}}}{2k_B T}.$$

Note that both species are equally abundant and that their partial pressures are thus half the total pressure. At $p_{\mathrm{tot}} = 1 \times 10^{-8}$ Pa we have the conditions of *ultrahigh vacuum* (UHV). We obtain $\mathscr{N}_{\mathrm{He}} = \mathscr{N}_{\mathrm{Xe}} = \mathscr{N} = 1.22 \times 10^{12}\,\mathrm{m}^{-3}$. For p_{tot} 0.1 Pa, we have the conditions of *medium vacuum*, where the particle densities take a value of $1.22 \times 10^{19}\,\mathrm{m}^{-3}$. Under the conditions of atmospheric pressure, we have $\mathscr{N} = 1.22 \times 10^{25}\,\mathrm{m}^{-3}$.

Equations for the collision rates and the mean free path were provided in Sect. 7.1.3. Collisions may occur between helium and helium, xenon and xenon, and helium and xenon. The cross-sections for these collisions can be estimated using the *hard sphere* model (Fig. 7.2) and the given van der Waals radii. If d_{AB} is the sum of the radii of two collision partners A and B, then the hard sphere collision cross-section is $\sigma_{\mathrm{AB}} = \pi d_{\mathrm{AB}}^2$. Thus,

$$\sigma_{\mathrm{He\,Xe}} = \pi\,(r_{\mathrm{He}} + r_{\mathrm{Xe}})^2 = 3.982 \times 10^{-19}\,\mathrm{m}^2.$$

In the same way, we obtain $\sigma_{\mathrm{He\,He}} = 2.463 \times 10^{-19}\,\mathrm{m}^2$ and $\sigma_{\mathrm{Xe\,Xe}} = 5.863 \times 10^{-19}\,\mathrm{m}^2$.

In the next step, we need to calculate the effective masses needed in turn for the evaluation of the mean relative velocities (Eq. (7.7)). From the periodic system of the elements we take the atomic weights 4.00 amu for helium, and 131.29 amu for xenon. Thus, we have $\mu_{\mathrm{He\,Xe}} = \frac{m_{\mathrm{He}} m_{\mathrm{Xe}}}{m_{\mathrm{He}} + m_{\mathrm{Xe}}} = 3.88$ amu, $\mu_{\mathrm{He\,He}} = 2$ amu, and $\mu_{\mathrm{Xe\,Xe}} = 65.65$ amu respectively. From the appendix Sect. A.1, we take the value of one atomic mass unit, $1\ \mathrm{amu} = 1.660538921(73) \times 10^{-27}\,\mathrm{kg}$. For room temperature (298 K) we obtain the mean relative velocity for helium:

$$\langle v_{\mathrm{He\,He}} \rangle = \left(\frac{8 k_B T}{\pi \mu_{\mathrm{He\,He}}} \right)^{\frac{1}{2}} = \left(\frac{8 \times 1.38065 \times 10^{-23}\,\mathrm{J\,K^{-1}} \times 298\,\mathrm{K}}{\pi \times 2 \times 1.66054 \times 10^{-27}\,\mathrm{kg}} \right)^{\frac{1}{2}} = 1776\,\mathrm{m\,s^{-1}}.$$

In the same way, we obtain $\langle v_{\mathrm{Xe\,Xe}}\rangle = 310\,\mathrm{m\,s^{-1}}$, and $\langle v_{\mathrm{He\,Xe}}\rangle = 1275\,\mathrm{m\,s^{-1}}$. The individual collision rates z_{AB} can be evaluated using Eq. (7.6):

$$z_{\mathrm{AB}} = \sigma_{\mathrm{AB}}\langle v_{\mathrm{AB}}\rangle \mathscr{N}$$

where $\mathscr{N}$ is the particle density of the collision partner. Inserting the cross-sections, mean relative velocities and particle densities, we obtain $z_{\mathrm{He\,He}} = 5.33 \times 10^{-4}\,\mathrm{s^{-1}}$ under ultrahigh vacuum conditions, $5.33 \times 10^{3}\,\mathrm{s^{-1}}$ under medium vacuum, and $5.33 \times 10^{9}\,\mathrm{s^{-1}}$ at atmospheric pressure. Similarly, for collisions among xenon atoms, we have $z_{\mathrm{Xe\,Xe}} = 2.22 \times 10^{-4}\,\mathrm{s^{-1}}$, $2.22 \times 10^{3}\,\mathrm{s^{-1}}$, and $2.22 \times 10^{9}\,\mathrm{s^{-1}}$ for UHV, medium vacuum, and atmospheric pressure respectively. For collisions of helium and xenon we obtain $z_{\mathrm{He\,Xe}} = 6.19 \times 10^{-4}\,\mathrm{s^{-1}}$, $6.19 \times 10^{3}\,\mathrm{s^{-1}}$, and $6.19 \times 10^{9}\,\mathrm{s^{-1}}$ for UHV, medium vacuum, and atmospheric pressure respectively.

Having obtained these collision rates, we can determine the mean free path for both species under the various conditions according to Eq. (7.8):

$$\lambda_{\mathrm{He}} = \frac{\langle v_{\mathrm{He}}\rangle}{z_{\mathrm{He\,He}} + z_{\mathrm{He\,Xe}}} \tag{7.42}$$

$$\lambda_{\mathrm{Xe}} = \frac{\langle v_{\mathrm{Xe}}\rangle}{z_{\mathrm{Xe\,Xe}} + z_{\mathrm{He\,Xe}}} \tag{7.43}$$

The mean velocities of helium and xenon are calculated using Eq. (7.16) and the respective atomic masses: $\langle v_{\mathrm{He}}\rangle = 1256\,\mathrm{m\,s^{-1}}$, $\langle v_{\mathrm{Xe}}\rangle = 219\,\mathrm{m\,s^{-1}}$. The resulting values for λ_{He} and λ_{Xe} at various pressures can be found in Table 7.2.

Under all pressure conditions, helium has a fourfold larger mean free path than xenon. Under ultrahigh vacuum conditions (10^{-8} Pa), the mean free paths are very large, much larger than the extension of every vacuum recipient. At 10^{-1} Pa, however, the mean free paths have values that are comparable with the tube diameters of vacuum equipment. It is worth mentioning that in fluid mechanics, the so-called *Knudsen number*

$$\mathrm{Kn} = \frac{\lambda}{l} \tag{7.44}$$

is used to characterize the flow within vacuum components of extension l by comparison with the mean free path. Under ambient pressure conditions (10^{5} Pa), the mean free path is within the submicrometer range. Under such conditions, collisions between particles markedly influence spectroscopic line profiles (colli-

Table 7.2 Mean free path of helium and xenon in a 50:50 mixture at room temperature and various pressure conditions

Pressure (Pa)	λ_{He} (m)	λ_{Xe} (m)
10^{-8}	1.09×10^{6}	2.6×10^{5}
10^{-1}	1.09×10^{-1}	2.6×10^{-2}
10^{5}	1.09×10^{-7}	2.6×10^{-8}

sional broadening). Another application is related to the above-mentioned transport processes, e.g., heat conduction. To be efficient, heat conduction requires many collisions between gas particles. In an ultrahigh vacuum where the mean free path exceeds the typical extensions of vacuum equipment by orders of magnitude, heat conduction mediated by particle collisions is thus largely suppressed. Under these conditions, heat transfer based on radiation is the only effective process. In Problem 9.3 this situation is considered in more detail.

Problem 7.5 (Gas Effusion) Consider a perfect gas in equilibrium at a temperature of T. Through a small sharp-edged orifice of area A gas effuses from the compartment into a vacuum if a shutter is opened (see Fig. 7.7). The particle density is so low that the mean free path is large compared with the orifice diameter. A particle detector is situated at a distance d in axial alignment with the orifice.

a. Starting from the Maxwell-Boltzmann distribution function (Eq. (7.1)), show that the velocity distribution function of the effusing molecular beam is

$$\frac{dN(v)}{N} = \frac{m^2}{2k_B^2T^2}\exp\left(-\frac{mv^2}{2k_BT}\right)v^3\,dv \tag{7.45}$$

N is the number of particles in the beam, and $dN(v)$ is the number of particles with velocity between v and $v + dv$.

b. Based on Eq. (7.45) derive a distribution function for the kinetic energy in the beam (see Problem 7.2). What is the mean kinetic energy in the molecular beam leaving the cell? Why are these distribution functions different from the Maxwell-Boltzmann functions?

c. Based on Eq. (7.45) derive an expression for the time-of-flight (TOF) distribution function of particles arriving at the detector at a time t after the shutter was opened for a very short time, negligible compared with the TOF. Assume neon at a temperature of 400 K and calculate the arrival of the TOF peak at $d = 0.5$, 1.0, and 1.5 m. Also, calculate the vertical shift of the beam due to gravitation.

Solution 7.5 In this exercise, we work out the principle of a simple method of molecular beam formation: effusion. The so-called **Knudsen effusion cells** are widely used in molecular beam epitaxy to grow thin films on surfaces or to investigate molecular beam reactive scattering in surface catalysis.

In **subproblem (a)**, our aim is to establish the velocity distribution of the particles emitted through the orifice. Equation (7.45) is not identical to the Maxwell-Boltzmann velocity distribution, as would perhaps be expected at first sight. To see

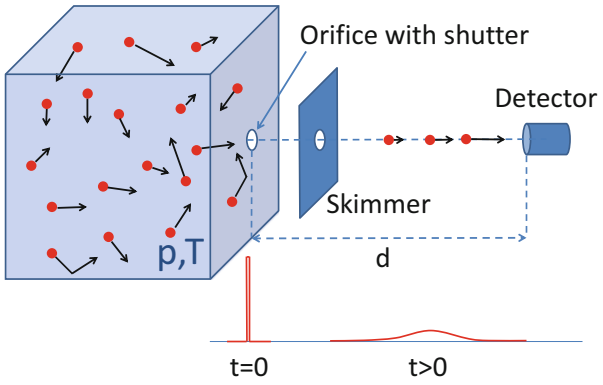

Fig. 7.7 Sketch of an effusion cell experiment with an axially aligned particle detector analyzing the molecular beam. The skimmer selects only particles moving in an axial direction

this, we have to recapitulate the derivation of the total impingement rate on a surface area element dA, which is part of the orifice area. All particles impinging on this area leave the compartment if the shutter is opened. Because the mean free path is larger than the orifice extension, we can assume that there will be no collisions among the particles. Hence, a particle with velocity between v and $v + dv$ coming from a direction characterized by a polar angle between θ and $\theta + d\theta$ and an azimuthal angle between ϕ and $\phi + d\phi$ leaves the orifice with only these values. Using results from Problem 7.1, we use the Maxwell-Boltzmann distribution in spherical coordinates:

$$\frac{dN(v,\theta,\phi)}{N_{\text{tot}}} = \left(\frac{m}{2\pi k_B T}\right)^{\frac{3}{2}} \exp\left(-\frac{mv^2}{2k_B T}\right) v^2 \sin\theta \, dv \, d\theta \, d\phi \tag{7.46}$$

This gives us the effective number of particles with only this particular velocity and direction. If we put the origin in the center of the surface element dA as illustrated in Fig. 7.8, we can narrow down the number of particles that hit the surface element within the time dt. First, the polar angle θ must take values between 0 (perpendicular impingement) and $\frac{\pi}{2}$ (extreme grazing incidence). Second, dependent on its velocity, the distance a particle moves within a time interval between t and $t + dt$ is $v\,dt$. Hence, a particle with this speed only hits the surface element if it is within the prism volume shown in Fig. 7.8. Its volume is $dV = v\cos(\theta)\,dt\,dA$. The number of particles with speed v and direction within this prism is therefore:

$$dN(v,\theta,\phi) = \frac{N_{\text{tot}}}{V}\left(\frac{m}{2\pi k_B T}\right)^{\frac{3}{2}} \exp\left(-\frac{mv^2}{2k_B T}\right) v^2 \sin\theta \, dv \, d\theta \, d\phi \underbrace{\frac{dV}{v\,dt\,dA\cos\theta}}, \tag{7.47}$$

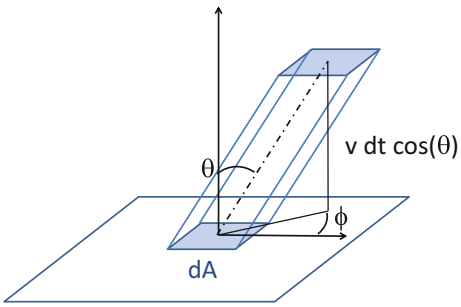

Fig. 7.8 Derivation of the number of particles with velocity between v and $v + dv$ impinging on a surface area element dA within the time interval between t and $t + dt$ from a polar angle between θ and $\theta + d\theta$ and an azimuthal angle between ϕ and $\phi + d\phi$

where V is the compartment volume and $\frac{N_{\text{tot}}}{V}$; thus, the number density $\mathcal{N}$. If we integrate this expression, we obtain the total impingement rate:

$$\begin{aligned}\frac{N}{dA\,dt} &= \int_0^\infty dv \int_0^{2\pi} d\phi \int_0^{\frac{\pi}{2}} d\theta\, \mathcal{N} \left(\frac{m}{2\pi k_B T}\right)^{\frac{3}{2}} \mathrm{e}^{-\frac{mv^2}{2k_B T}} v^3 \sin\theta \cos\theta \\ &= \mathcal{N} \left(\frac{m}{2\pi k_B T}\right)^{\frac{3}{2}} \underbrace{\int_0^\infty \mathrm{e}^{-\frac{mv^2}{2k_B T}} v^3\, dv}_{\overset{\text{Eq. (A.48)}}{=} 2\left(\frac{k_B T}{m}\right)^2} \underbrace{\int_0^{2\pi} d\phi}_{=2\pi} \underbrace{\int_0^{\frac{\pi}{2}} \sin\theta \cos\theta\, d\theta}_{\overset{\text{Eq. (A.41)}}{=} \frac{1}{2}} \\ &= \mathcal{N} \left(\frac{k_B T}{2\pi m}\right)^{\frac{1}{2}}\end{aligned}$$

which is in accordance with Eq. (7.9). If we omit in the last step the integration over the velocity, we obtain the impingement rate of all particles with velocities between v and $v + dv$:

$$\frac{dN(v)}{dA\,dt} = \pi \mathcal{N} \left(\frac{m}{2\pi k_B T}\right)^{\frac{3}{2}} \mathrm{e}^{-\frac{mv^2}{2k_B T}} v^3\, dv \tag{7.48}$$

If we divide $\frac{dN(v)}{dA\,dt}$ by the total impingement rate obtained above, we obtain an expression for the velocity distribution:

$$\frac{dN(v)}{N} = \pi \frac{\left(\frac{m}{2\pi k_B T}\right)^{\frac{3}{2}}}{\left(\frac{k_B T}{2\pi m}\right)^{\frac{1}{2}}} e^{-\frac{mv^2}{2k_B T}} v^3\, dv = \frac{m^2}{2k_B^2 T^2} e^{-\frac{mv^2}{2k_B T}} v^3\, dv \tag{7.49}$$

which is simply Eq. (7.45). The distribution function is normalized, which is easily seen if we integrate it over the entire velocity range using Eq. (A.48) from the integral table. The essential difference between this velocity distribution and the Maxwell-Boltzmann distribution Eq. (7.46) is the cubic factor for velocity. Therefore, compared with the Maxwell-Boltzmann distribution valid for the gas

particles within the effusion cell volume, more particles with higher velocity reach the orifice and are emitted if the shutter is opened. Thus, the velocity distribution of the particles leaving the cell through the orifice is non-Maxwellian.

In **subproblem (b)**, we find the kinetic energy distribution compatible with Eq. (7.45), similar to what we have done for the Maxwell-Boltzmann distribution in problem 7.2. If $E = \frac{1}{2}mv^2$ is the kinetic energy and $p = mv$ the momentum of a particle, $dE = p\,dv$. Therefore, Eq. (7.45) can be written in the following way:

$$\frac{dN(v)}{N} = \frac{m}{k_B T}\frac{mv^2}{2k_B T v^2} e^{-\frac{mv^2}{2k_B T}} v^3 \underbrace{dv}_{\frac{dE}{p}}$$

$$= \frac{m}{k_B T}\frac{E}{k_B T}\underbrace{v}_{\frac{p}{m}}\frac{dE}{p}.$$

Thus,

$$\frac{dN(E)}{N} = \frac{1}{k_B T}\frac{E}{k_B T}\mathrm{e}^{-\frac{E}{k_B T}}\,dE. \tag{7.50}$$

We now scale the energy to the thermal energy introducing $\epsilon = \frac{E}{k_B T}$. With $dE = k_B T\,d\epsilon$ we obtain the simple expression

$$\frac{dN(\epsilon)}{N} = w(\epsilon) = \exp(-\epsilon)\,\epsilon\,d\epsilon. \tag{7.51}$$

Apparently, the kinetic energy distribution of molecular beam effusing through the orifice only depends on the temperature, and not on the particle mass. It is instructive to compare $w(\epsilon)$ with the corresponding function from the Maxwell-Boltzmann distribution (Eq. (7.20)) from Problem 7.2, i.e., with the kinetic energy distribution within the compartment.

Both functions are shown in Fig. 7.9. Already a qualitative inspection shows that the molecular beam leaving the compartment has a higher mean kinetic energy. This is consistent with our above interpretation of the velocity distribution function. We obtain the most probable kinetic energy $\epsilon_{\max}$ by setting the first derivative of $w(\epsilon)$ to zero:

$$\left.\frac{dw(\epsilon)}{d\epsilon}\right|_{\epsilon=\epsilon_{\max}} = \exp(-\epsilon_{\max})\left(1-\epsilon_{\max}^2\right) \stackrel{!}{=} 0$$

Thus, $\epsilon_{\max} = 1$. In Problem 7.2 we found $\epsilon_{\max} = \frac{1}{2}$ for the Maxwell-Boltzmann distribution. Thus, the most probable kinetic energy of the particles leaving the orifice, the peak of $w(\epsilon)$ in Fig. 7.9 is twice the peak value of the kinetic energy in the compartment. Furthermore, we calculate the mean kinetic energy $\langle\epsilon\rangle$ of the

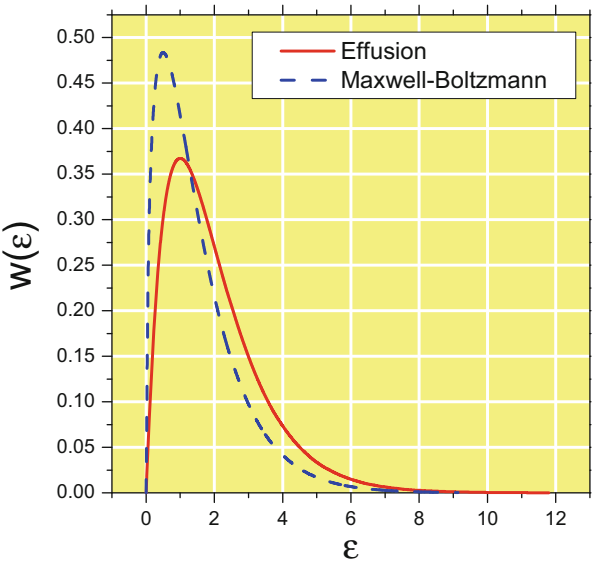

Fig. 7.9 Comparison between the kinetic energy distribution function of a molecular beam leaving the effusion cell (*solid line*) and the kinetic energy distribution within the compartment (*dashed line*, see Problem 7.2)

particles in the molecular beam. This is:

$$\langle \epsilon \rangle = \int_0^\infty \epsilon \, w(\epsilon) \, d\epsilon = \int_0^\infty \epsilon^2 \mathrm{e}^{-\epsilon} \, d\epsilon$$
$$\overset{\text{Eq. (A.44)}}{=} \mathrm{e}^{-\epsilon} \left(-\epsilon^2 + 2\epsilon - 2 \right) \Big|_0^\infty = 2$$

Hence, the mean kinetic energy of the particles in the molecular beam at a given temperature is $2k_BT$. Again, this value is larger than the mean kinetic energy of the particles in the compartment of $\frac{3}{2}k_BT$ (see Eq. (7.18) in Problem 7.1).

In **subproblem (c)** we deal with the TOF of a pulse of particles leaving the compartment if the shutter is opened instantaneously for a very short period at time $t = 0$. The situation is shown in Fig. 7.7. We can assume that the particle beam at $t = 0$ is a *delta* peak, i.e., an arbitrarily sharp peak. Because faster particles need a shorter time to cover the distance between the orifice and the detector than slower ones, the pulse expands and thus changes its profile. To determine the TOF profile, we must transform the velocity distribution into a TOF distribution. If d is the distance covered by a particle arriving between time t and $t + dt$, its velocity is $v = \frac{d}{t}$ and thus $dv = -\frac{d}{t^2} dt$. Therefore, we can rewrite

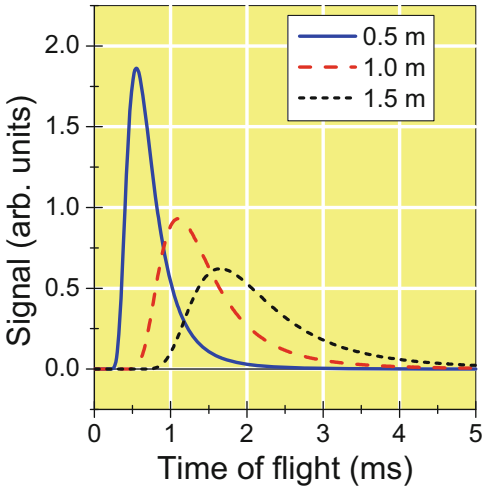

Fig. 7.10 Time of flight distribution of a group of particles at different distances from the detector

Eq. (7.45):

$$\frac{dN(v(t))}{N} = -\frac{m^2}{2k_B^2T^2}\exp\left[-\frac{m}{2k_BT}\left(\frac{d}{t}\right)^2\right]\left(\frac{d}{t}\right)^3\frac{d}{t^2}\,dt \tag{7.52}$$

The negative sign compensates for the fact that an increase in velocity by a positive dv involves a negative dt. Defining a parameter $\alpha = \sqrt{\frac{m}{2k_BT}}$, we use the last expression to obtain the rate at which particles arrive at the detector at a given time t:

$$\frac{dN(t)}{dt} = -\frac{2Nd^4}{\alpha^4t^5}\exp\left(-\frac{d^2}{\alpha^2t^2}\right) \tag{7.53}$$

The detector counts the incoming particles per period of time; thus, we assume that the detector signal is proportional to this rate.[2] Thus, the detector signal, $S(t)$, is:

$$S(t) = c\frac{d^4}{\alpha^4t^5}\exp\left(-\frac{d^2}{\alpha^2t^2}\right), \tag{7.54}$$

where c is a constant. $S(t)$ is plotted in Fig. 7.10 for the case of neon (atomic mass $m = 20.18$ amu), a temperature of 400 K, and three different distances. With increasing distance, the TOF profile becomes broader and its maximum moves, as expected, to longer arrival times. We could look up the respective peak values or obtain an expression for the position t_{max} of the TOF peak at which the first

[2] In practice, the detector sensitivity is a function of the velocity, with the tendency to decrease as v increases.

derivative of $S(t)$ becomes zero:

$$S(t_{\max}) = c\frac{d^4}{\alpha^4 t_{\max}^5}\exp\left(-\frac{d^2}{\alpha^2 t_{\max}^2}\right)\left[\frac{2d^2}{\alpha^2 t_{\max}^8} - \frac{5}{t_{\max}^6}\right] \stackrel{!}{=} 0 \tag{7.55}$$

We thus obtain:

$$t_{\max} = \sqrt{\frac{2}{5}}\frac{d}{\alpha} \tag{7.56}$$

With $\alpha = 574.12$ for the given conditions, we thus locate the TOF peaks at 0.55 ms for $d = 0.5$ m, 1.10 ms for $d = 1.0$ m, and 1.65 ms for $d = 1.5$ m, corresponding to a velocity of 909 m s^{-1}. Finally, it is instructive to check whether gravitational effects have a significant influence on the trajectories of the particles between shutter and detector. Given the gravity acceleration of $g = 9.81\,\mathrm{m\,s^{-2}}$, the vertical shift after the time t is given by $y = \frac{1}{2}gt^2$. If we insert the above values for the TOF, we obtain a vertical shift of 1.5×10^{-6} m at distance of 0.5 m, 5.9×10^{-6} m at $d = 1$ m, and 1.3×10^{-5} m at $d = 1.5$ m. Gravitational effects are therefore negligible under these conditions.

Problem 7.6 (Film Growth) Water vapor (partial pressure of 1×10^{-5} Pa, gas temperature 300 K) condenses on a cold surface and freezes as amorphous ice (density $\rho = 0.94\,\mathrm{g\,cm^{-3}}$). If each molecule impinging on the surface sticks to it, how long does it take to grow an ice film 1 μm thick?

Solution 7.6 In this exercise, we deal with the growth of an amorphous ice film on a cold surface. Within kinetic theory, it is possible to include time in considerations of changes of state—a point that is excluded in an analysis based on thermodynamics in Chap. 3. The goal is to calculate the time t to grow an ice film 1 μm thick on a cold surface, given the gas phase partial pressure p and temperature T. The problem is a simple application of the relation of the impingement rate Eq. (7.10), which gives the relation between the number of particles impinging on a surface per second and per m^2, and the gas temperature and partial pressure of the particles. We may assume that each particle that hits the surface sticks to it—an assumption that in the case of ice is valid at cryogenic temperature below 100 K. Under these conditions H_2O freezes as amorphous ice (see Fig. 7.11). At first, we calculate the number of H_2O molecules forming a $d = 1$ μm thick ice film with an area of, say, $A = 1\,\mathrm{m^2}$. Because the density is

$$\rho = \frac{m}{V} = \frac{m}{A\,d}, \tag{7.57}$$

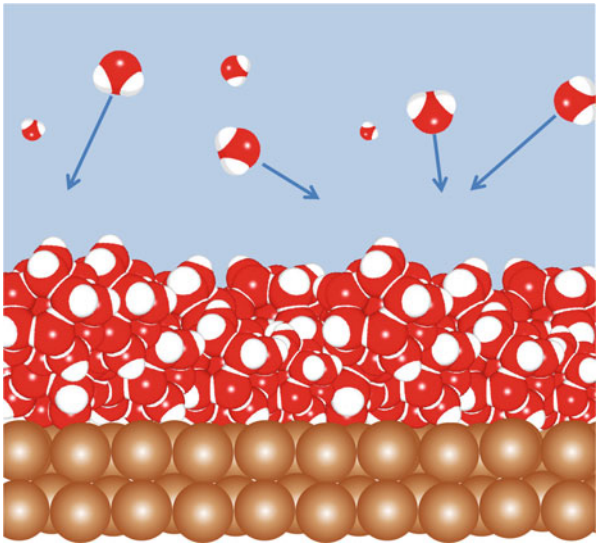

Fig. 7.11 Water molecules impinging on a surface form a film of amorphous ice

this film has the mass $m = \rho A\, d$, corresponding to an amount

$$n = \frac{m}{M_{H_2O}} = \frac{\rho A\, d}{M_{H_2O}} \tag{7.58}$$

and thus a particle number of

$$N = \frac{N_A \rho A\, d}{M_{H_2O}} \tag{7.59}$$

where $M_{H_2O} = 18\,\mathrm{g\,mol^{-1}}$ is the molar mass of water and N_A is the Avogadro constant. Given an impingement rate

$$I = \frac{p}{\sqrt{2\pi m_{H_2O} k_B T}} = \frac{N}{A\, t}, \tag{7.60}$$

the time sought is

$$t = \frac{N_A \rho\, d}{M_{H_2O}} \frac{\sqrt{2\pi m_{H_2O} k_B T}}{p} \tag{7.61}$$

With a mass $m_{H_2O} = 2.989 \times 10^{-26}\,\mathrm{kg}$ of the water molecule and $\rho = 940\,\mathrm{kg\,m^{-3}}$ we obtain the result $t = 87{,}712\,\mathrm{s}$, i.e., under the given conditions a film thickness of $1\,\mu\mathrm{m}$ is reached after more than 24 h.